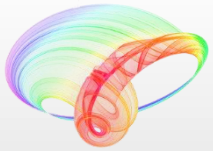

Photonica2021

VIII International School and Conference on Photonics
August 23 - August 27, 2021, Belgrade, Serbia

High-resolution terahertz and infrared spectroscopy of hybrid perovskite $CH_3NH_3PbI_3$

V. Anikeeva[1,2], K. Boldyrev[1], O. Semenova[3], and M. Popova[1]

[1]Institute of Spectroscopy of the Russian Academy of Sciences, Troitsk, Moscow, Russia

[2]National Research University Higher School of Economics, Moscow, Russia

[3]Rzhanov Institute of Semiconductor Physics of the Siberian Brunch of the Russian Academy of Sciences, Novosibirsk, Russia

e-mail: vanikeeva@hse.ru

Introduction

The growing interest in the study of hybrid metal halide perovskites $MAPbX_3$ ($MA = CH_3NH_3^+$, X = I, Br, Cl) as new materials for use in solar cells and photovoltaic devices is due to such excellent optoelectronic properties [1] as:

- extremely high luminescence efficiency;
- optimal band gap: *1.55 eV*;
- high value of the diffusion length of charge carriers: *175 μm*;
- absorption coefficient: *10^5 cm^{-1}*;

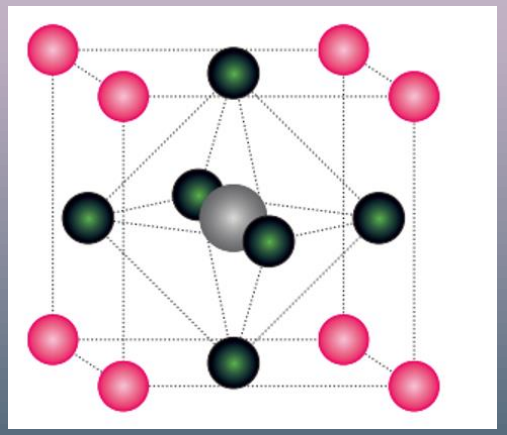

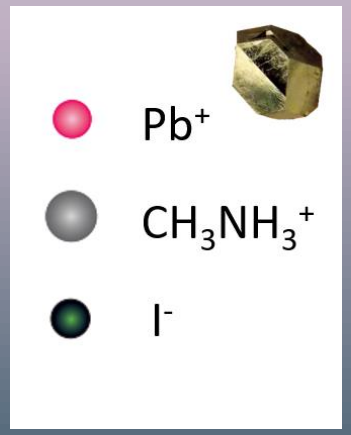

Structure of organometallic perovskite $CH_3NH_3PbI_3$.

Many of these functional properties are closely related to the features of the phonon spectrum and the electron-phonon interaction.
Notwithstanding a large number of studies of optical properties of hybrid perovskites, most of them were carried out on thin films. In this work, high quality large single crystals of methyl ammonia lead iodide ($CH_3NH_3PbI_3$) were investigated by high-resolution (up to 0.2 cm^{-1}) spectroscopy in the wide spectral (15 – 650 cm^{-1}, 1750 – 12000 cm^{-1}) and temperature (5 – 330 K) ranges.

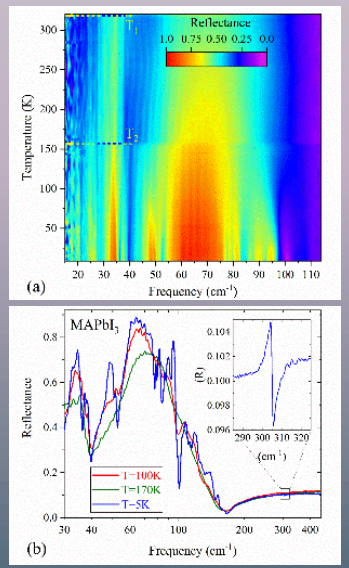

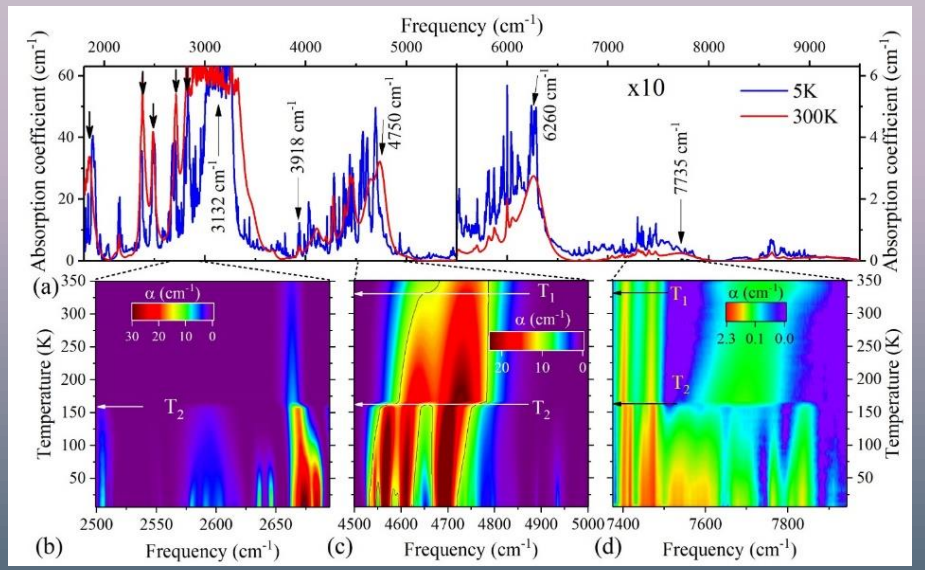

[1] M. R. Filip, Handbook of Materials Modeling (Springer, Cham), 1, (2018).

Motivation

Hybrid organometallic perovskites applications

Devices based on perovskite [2]

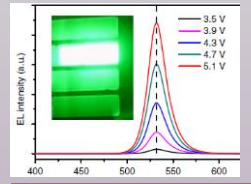

LEDs [3]

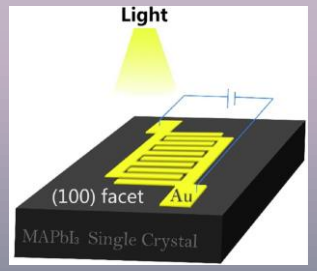

Lasers [6]

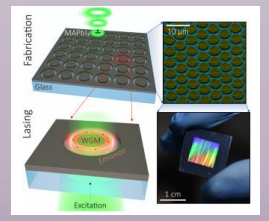

Photodetectors [7]

Solar cells [4]

[2] F. Brivio, J. M. Frost, J. M. Skelton, et. al., Phys. Rev. B: Condens. Matter Mater. Phys., 92, 144308, (2015).
[3] Z.-K. Tan, R. S. Moghaddam, M. L. Lai, et al., Nature Nanotech 9, 687–692 (2014).
[4] T. Brenner, D. Egger, L. Kronik, G. Hodes, D. Cahen, Nat. Rev. Mater. 1, 15007 (2016).
[6] A. Zhizhchenko, S. Syubaev, A. Berestennikov, et al., ACS Nano 13, 4, 4140, (2019).
[7] Z. Lian, Q. Yan, Q. Lv, et al., Scientific Reports, 5, 16563 (2015).

Importance of researching a single crystal form

Currently, perovskite thin films are being intensively studied, and most of the claimed applications are focused specifically on polycrystalline thin films. Accordingly, many recent reviews regarding progress in perovskites focus on their form of polycrystalline film. However, the study of the fundamental properties of organometallic perovskites should be carried out precisely on single crystals because of their low density of traps and the absence of grain boundaries. In addition, recent studies have shown that perovskite single crystals have much better optoelectronic properties than their polycrystalline film analogues [8].

Best research-cell efficiencies [5]

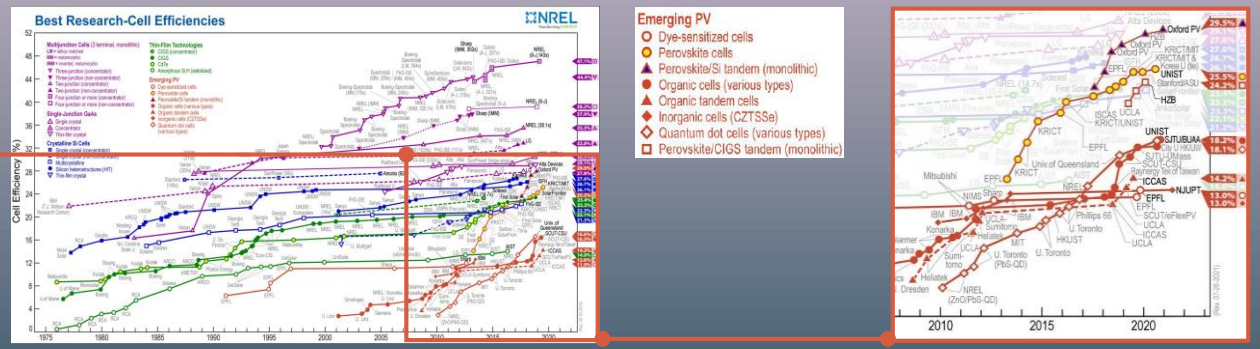

[5] NREL https://www.nrel.gov/pv/cell-efficiency.html.
[8] J. Ding, Q. Yan, Sci. China Mater. **60**, 1063–1078 (2017).

$CH_3NH_3PbI_3$ structural phase transitions

[1]

Cubic

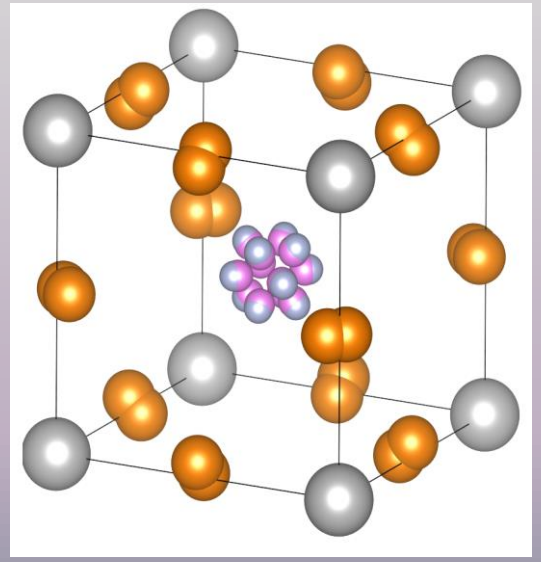

> 327 K

T_1=327 K

Tetragonal

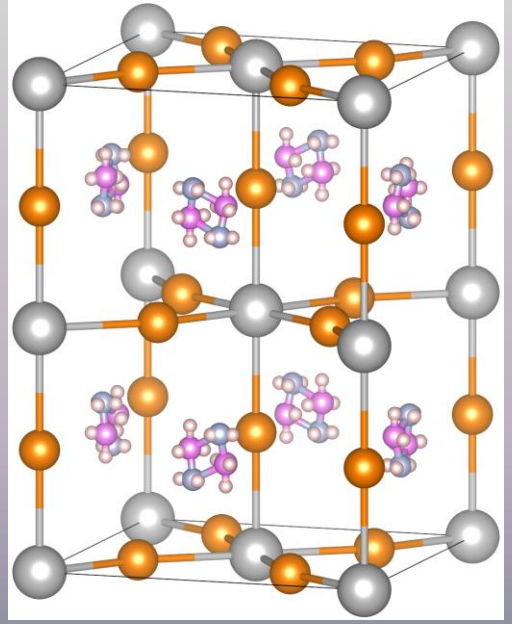

327 K < T < 161 K

T_2=160 K

Orthorhombic

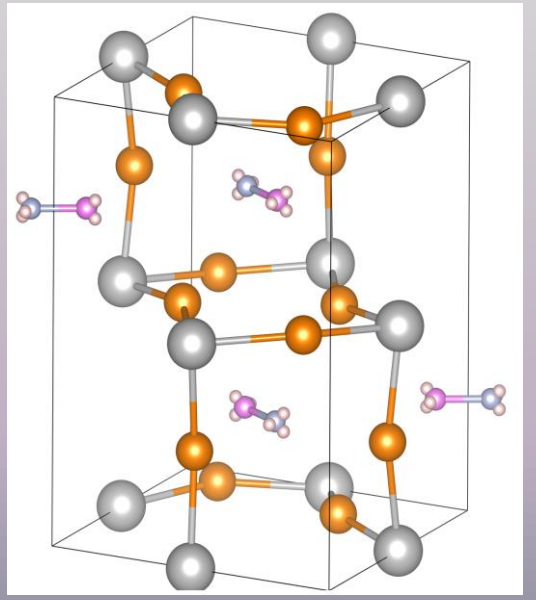

< 160 K

[1] M. R. Filip, Handbook of Materials Modeling (Springer, Cham), 1, (2018).

Three well-separated frequency regions of vibrations

[2]

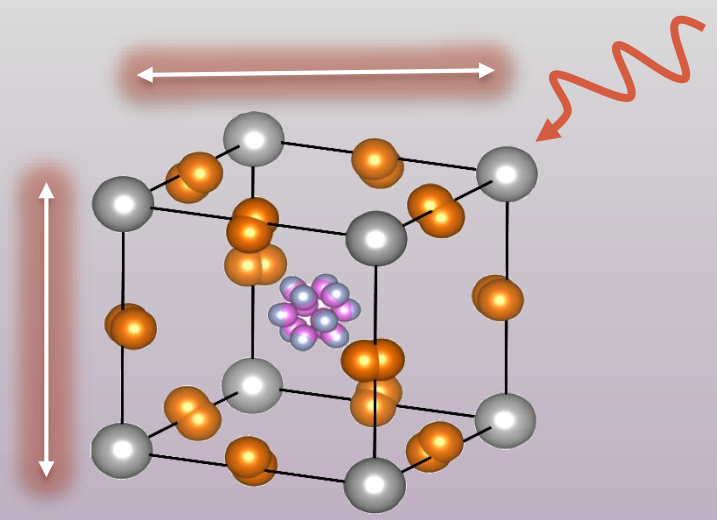

15 – 100 cm^{-1}
vibrations of the PbI_3 network consisting of heavy atoms and translational /librational modes of the MA cation

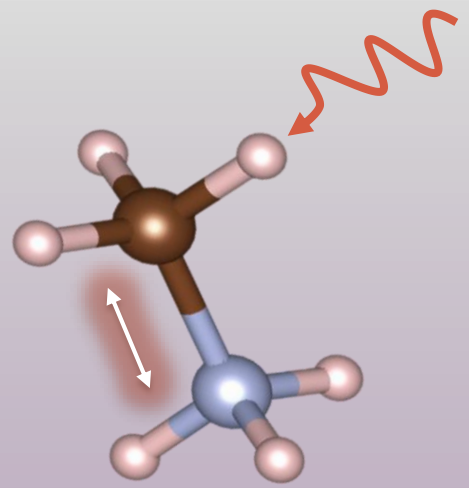

900 – 1600 cm^{-1}
CH_3NH_3 rocking modes, C−N stretching, and CH_3 and NH_3 bending vibrations

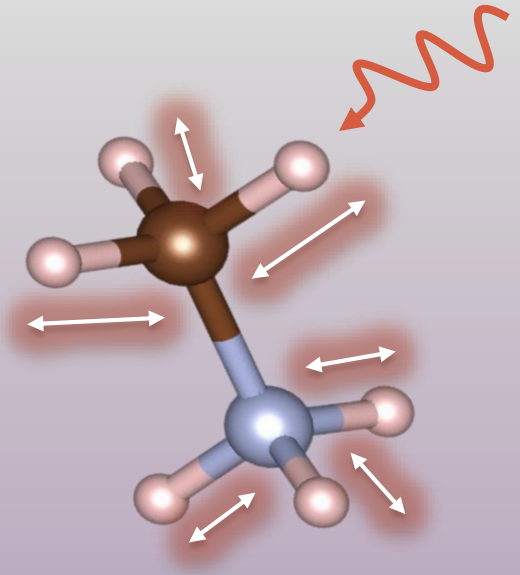

3000 and 3200 cm^{-1}
C−H and N−H stretching mode

In this work the reflection spectra in terahertz region and transmission spectra in the mid- and near-infrared (IR) regions of $CH_3NH_3PbI_3$ are studied for the first time for single crystals with the aim of obtaining information about low-frequency phonons and multiphonon lattice excitations that was not obtained by previously used experimental techniques or/and samples.

[2] F. Brivio, J. M. Frost, J. M. Skelton, et. al., Phys. Rev. B: Condens. Matter Mater. Phys., 92, 144308, (2015).

Synthesis

Sample preparation

1) CH_3NH_3I synthesis
2) PbI_2 synthesis

} Two precursors

3) $CH_3NH_3I + PbI_2 \longrightarrow CH_3NH_3PbI_3$

Synthesized single crystals.

Composition and structure

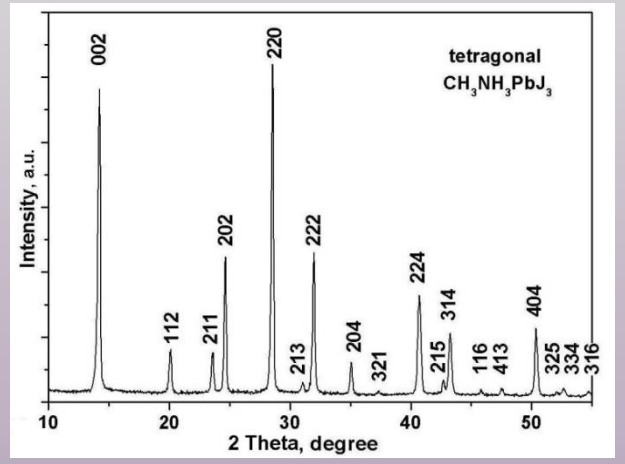

XRD pattern of the $CH_3NH_3PbI_3$ crystals.

Space group:
I4/mcm
Lattice constant:
a = 8.8743 Å, c = 12.6708 Å

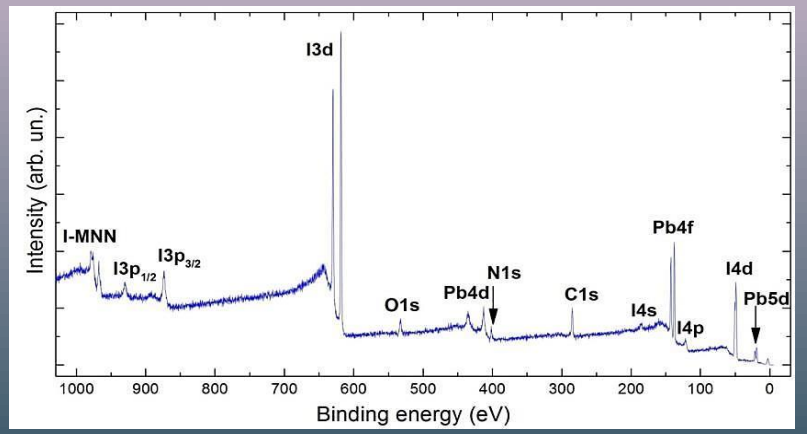

XPS spectrum of the $CH_3NH_3PbI_3$ single crystal surface.

[9] V. E. Anikeeva, O. I. Semenova, O. E. Tereshchenko, J. Phys.: Conf. Ser. 1124, 041008 (2018).
[10] O.I. Semenova, E.S. Yudanova, N.A. Yeryukov, et. al. Journal of Crystal Growth. 462, 45, (2017).
[11] E. S. Yudanova, T.A. Duda, O. E. Tereshchenko, O. I. Semenova, Journal of Structural Chemistry. 58, 8, 1567, (2017).

Experimental setup

Bruker IFS 125HR Fourier Spectrometer

The sample on a cryostat copper finger

Registration of reflection and absorption spectra: Bruker IFS 125HR Fourier Spectrometer
Range: 10 - 30000 cm^{-1}
Resolution: up to 0.2 cm^{-1}
Sample cooling: CryoMech ST403 closed loop cryostat (Temperature range: 3.5-300 K)

Results

Reflection spectra

$$\varepsilon(\omega) = \varepsilon_\infty + \sum_{i=1}^{N} \frac{\omega_{0i}^2 f_i}{\omega_{0i}^2 - \omega^2 + i\omega\gamma_i} \qquad R(\omega) = \left| \frac{\sqrt{\varepsilon(\omega)} - 1}{\sqrt{\varepsilon(\omega)} + 1} \right|^2$$

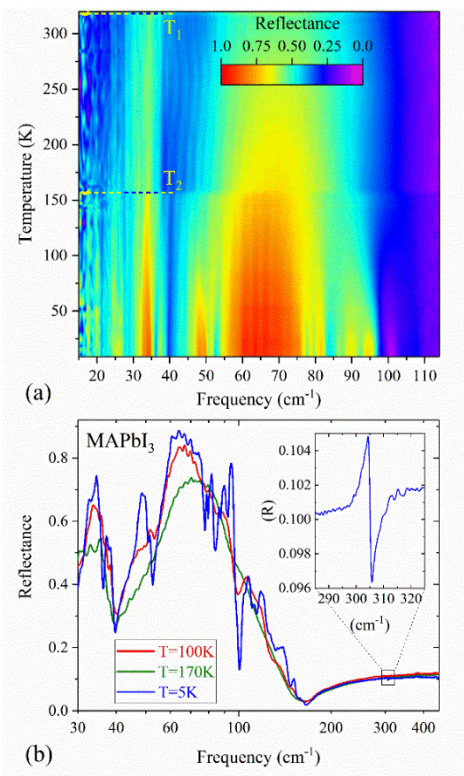

Reflection spectra of a $CH_3NH_3PbI_3$ single crystal (a) presented as the intensity map in the wave number – temperature axes and (b) at several selected temperatures. Horizontal arrows in (a) indicate structural phase transitions.

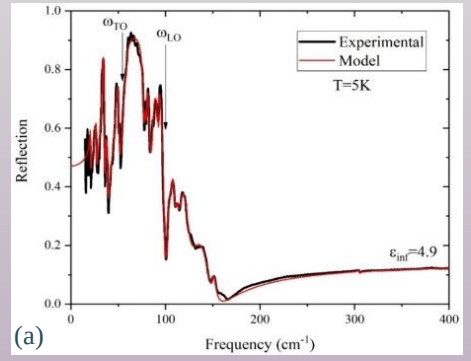

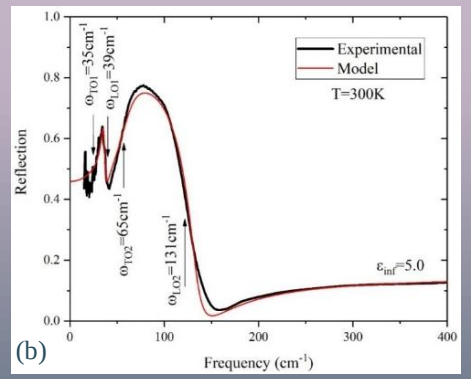

The reflection spectrum (black line) at 5 K (a) and 300 K (b) and the result of fitting by Eqs. (red dashed line).

Table 1. The frequencies ω_{TO} and ω_{LO} of the optical modes, observed in the far-IR spectra of $CH_3NH_3PbI_3$ at 5 K. ε_∞ = 4.9, ε_0 = 27.5

No	Ref. (12), 10K ω_{TO} (cm^{-1})	This work, 5 K		Tentative assignment
		ω_{TO} (cm^{-1})	ω_{LO} (cm^{-1})	
1	17	20.5	20.7	PbJ_6 octahedra twist
2	22	26.6	27.3	PbJ_6 octahedra twist
3	30	33.5	35.9	Pb–I–Pb rock
4	35	37.5	38.8	Pb–I–Pb rock
5	47	48.6	51.2	Pb−I−Pb bend
6	59	57.5	99.2	Pb–I–Pb stretch
7		78.0*	77.3	Pb−I−Pb bend
8		80.0*	79.6	Pb−I−Pb bend, $CH_3NH_3^+$ libr
9		85.9*	83.9	Pb−I−Pb bend, $CH_3NH_3^+$ libr
10		91.5*	91.3	$CH_3NH_3^+$ translation
11		92.8*	92.5	$CH_3NH_3^+$ translation
12		103.0	105.2	$CH_3NH_3^+$ libr/transl
13		106.3	110.0	$CH_3NH_3^+$ libr/transl
14		111.2	113.9	$CH_3NH_3^+$ rotation along C-N
15		116.0	126.1	
16		133.2	144.3	$CH_3NH_3^+$ libr/transl
17		150.1	152.6	$CH_3NH_3^+$ libr/transl
18		305.06	305.12	$CH_3NH_3^+$ torsion

(12) J. Phys. Chem. C 2015, 119, 25703

Results

Absorption spectra of a $CH_3NH_3PbI_3$ single crystal

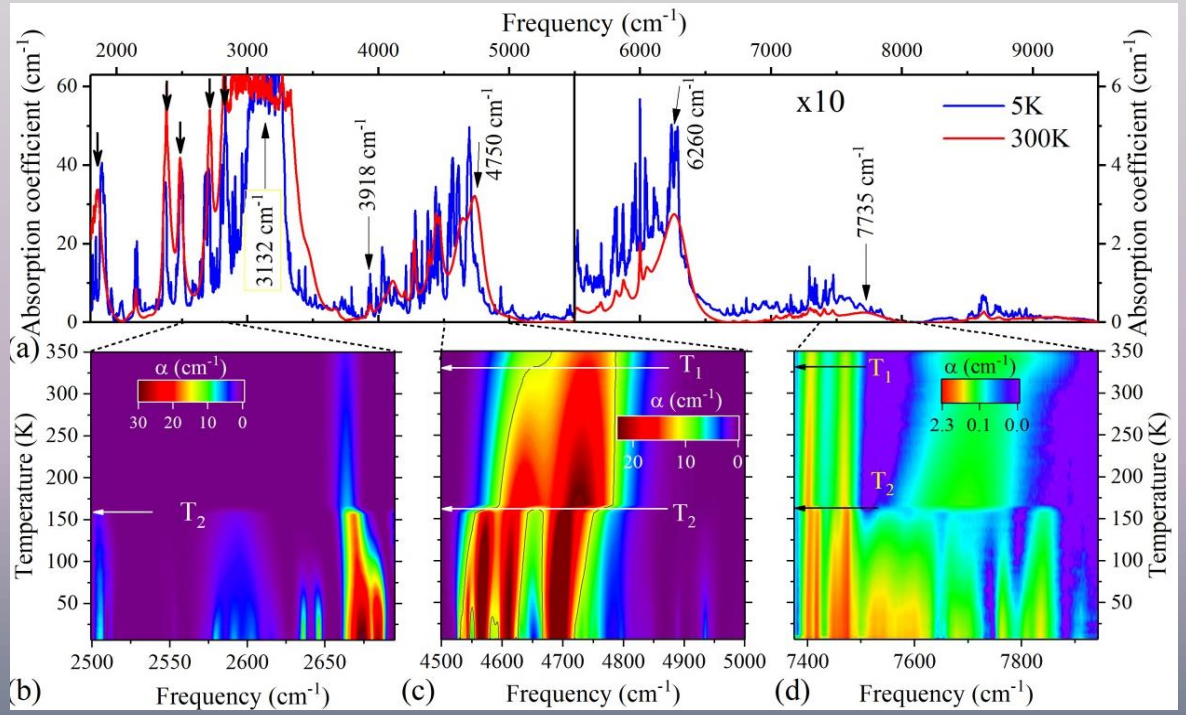

Absorption spectra (a) at the temperatures of 300 and 5 K; (b,c,d) presented as color intensity maps in the frequency – temperature axes for selected frequency regions. In (b), the contribution from the strong band at about 3000 cm^{-1} is subtracted. Temperatures T_1 and T_2 of the structural phase transitions are marked by horizontal arrows.

Different features in parameters of optical modes

Temperature dependences of the (a,e) integral intensity, (b,c,d) position, and (b,e) FWHH for (a,b) a singlet 3918 cm^{-1}; (c) a doublet near 2680 cm^{-1}; (d,e) a triplet near 2600 cm^{-1}. Below 70 K, the width of the central component of the triplet is presented. Inset of Fig. 3b shows a hysteresis for the line position at cooling and heating.

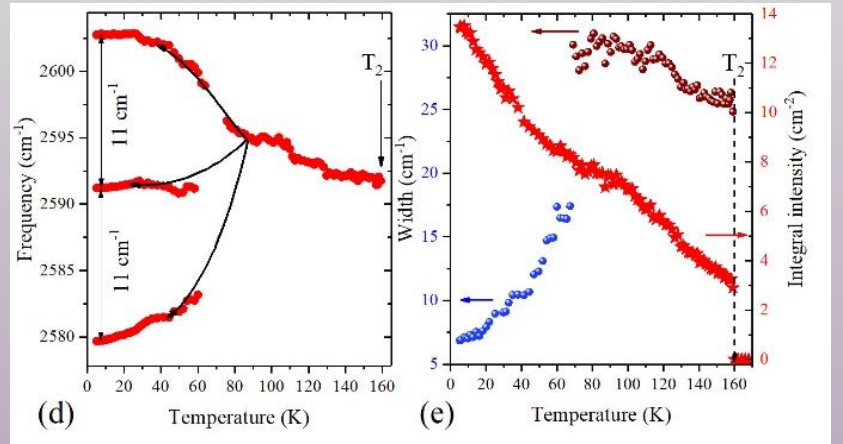

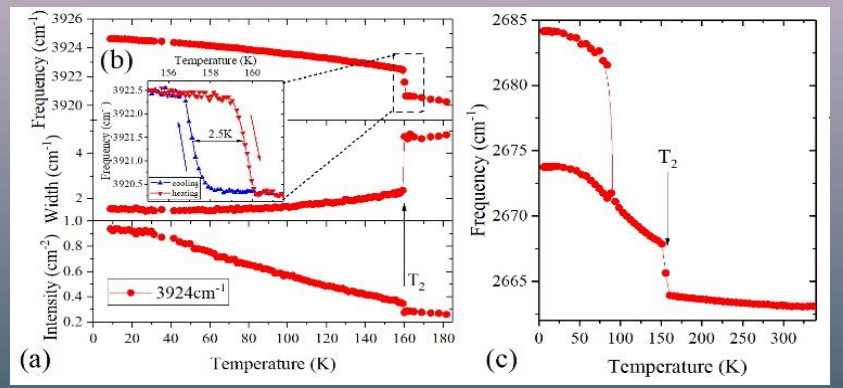

Results

Absorption spectra of a $CH_3NH_3PbI_3$ single crystal

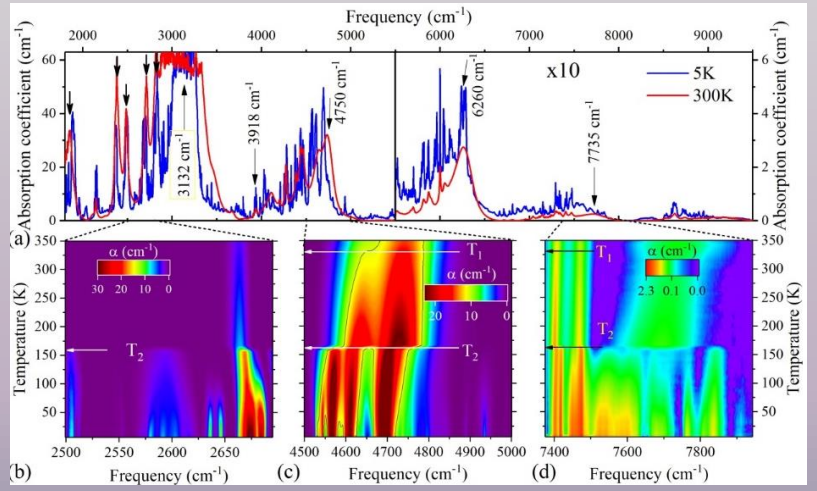

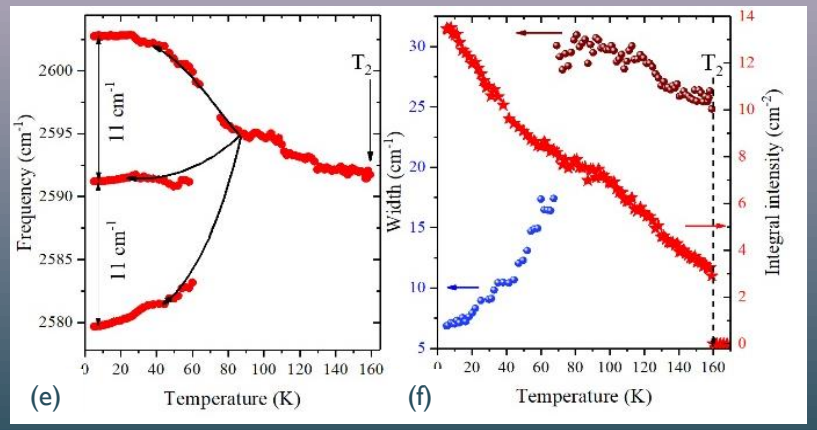

Multiphonon Spectra of $CH_3NH_3PbI_3$: Signatures of the Tunneling Dynamics of the $CH_3NH_3^+$ Cation

The line with the frequency 2592 cm^{-1} appears only below the temperature of the tetragonal to orthorhombic phase transition at T = 160 K (b). At about 70 K, this broad line splits into three equidistant (11 cm^{-1}) lines (e), which strongly narrow with further cooling (f).

The line can be tentatively assigned to a combination of the CH_3 symmetric bending vibration (1386 cm^{-1}), $CH_3NH_3^+$ rocking (906 cm^{-1}), and torsional (305 cm^{-1}) motions, but the observed splitting $\Delta\nu$ = 11 cm^{-1} could be the tunneling splitting due to rotational tunneling between three equivalent minima around the three equilibrium positions 0, $\pm 2\pi/3$ for the torsional vibration of the molecular cation.

The corresponding correlation time would be $\tau_{||} = 1/c\Delta\nu$ = 3 ps.

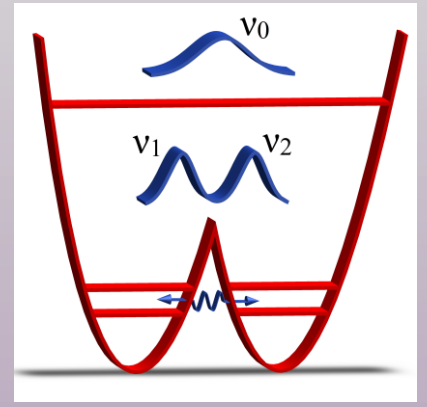

Conclusion

- The high-resolution terahertz (far-IR) reflection and mid- and near-infrared transmission studies of $CH_3NH_3PbI_3$ hybrid perovskite single crystals were performed in a broad range of temperatures (5−350 K).
- We observed 13 new low-frequency modes not reported previously and investigated the multiphonon spectra for the first time.
- There are only two modes of the inorganic cage (with frequencies of about 30 and 60 cm^{-1}) that survive in all structural phases of $CH_3NH_3PbI_3$. Their frequencies do not change at the phase transition from the cubic to tetragonal phase (320 K) but experience an abrupt shift at the tetragonal to orthorhombic transition (160 K).
- A high sensitivity to the structural phase transitions and to changes in the rotational dynamics of the $CH_3NH_3^+$ molecular cation is demonstrated also by the multiphonon spectra.
- Splitting of selected multiphonon lines observed below the temperature of ~70 K (identified earlier with a transition to the tunneling dynamics) is tentatively assigned to the tunneling splitting.
- A complete melting of the orientational order above the temperature of the orthorhombic to tetragonal phase transition leads to a noticeable broadening of vibrational lines.

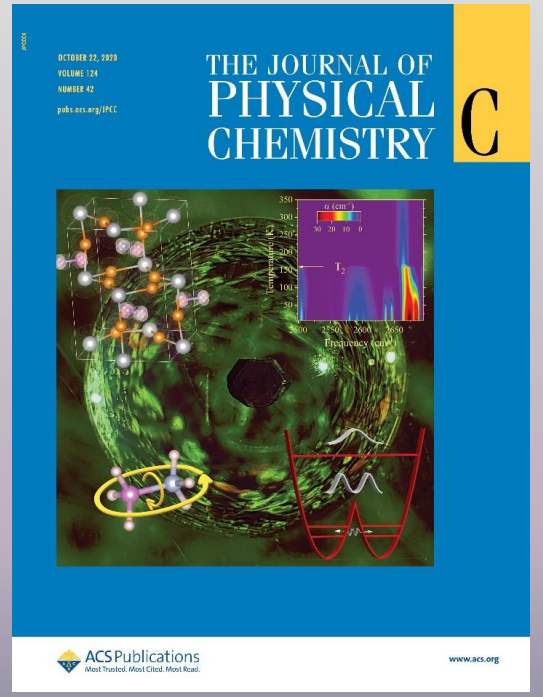

Infrared Spectra of the $CH_3NH_3PbI_3$ Hybrid Perovskite: Signatures of Phase Transitions and of Organic Cation Dynamics Kirill N. Boldyrev, Vasilisa E. Anikeeva, Olga I. Semenova, Marina N. Popova *J. Phys. Chem. C* 2020, 124, 42, 23307–23316

Thank you for attention!

e-mail: vanikeeva@hse.ru

Photonica2021

VIII International School and Conference on Photonics
August 23 - August 27, 2021, Belgrade, Serbia

HIGH-RESOLUTION TERAHERTZ AND INFRARED SPECTROSCOPY OF HYBRID PEROVSKITE $CH_3NH_3PbI_3$

V. Anikeeva[1,2], K. Boldyrev[1], O. Semenova[3], and M. Popova[1]
[1]Institute of Spectroscopy of the Russian Academy of Sciences, Troitsk, Moscow, Russia
[2]National Research University Higher School of Economics, Moscow, Russia
[3]Rzhanov Institute of Semiconductor Physics of the Siberian Brunch of the Russian Academy of Sciences, Novosibirsk, Russia
e-mail: vanikeeva@hse.ru

Introduction

The growing interest in the study of hybrid metal halide perovskites $MAPbX_3$ (MA = $CH_3NH_3^+$, X = I, Br, Cl) as new materials for use in solar cells and photovoltaic devices is due to such excellent optoelectronic properties [1] as:

- extremely high luminescence efficiency;
- optimal band gap: *1.55 eV*;
- high value of the diffusion length of charge carriers: *175 μm*;
- absorption coefficient: 10^5 *cm*$^{-1}$;

Best research-cell efficiencies

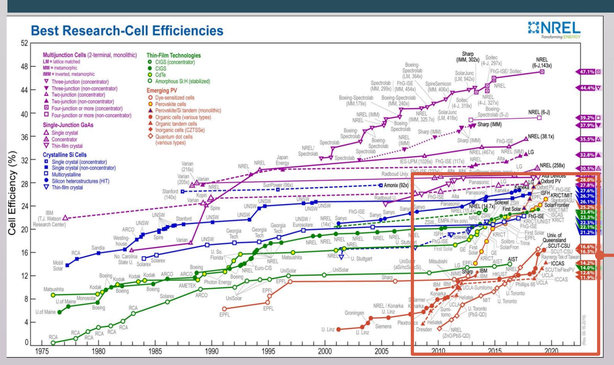

[3]

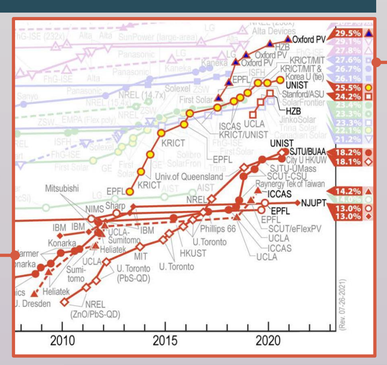

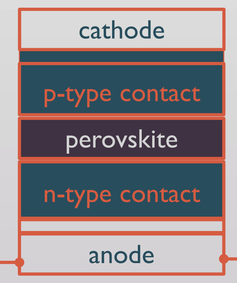

Devices based on perovskite [7]

LEDs [4]

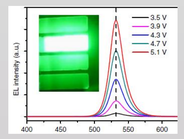

Lasers [5]

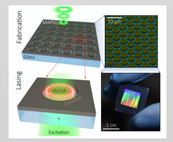

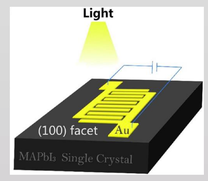

Solar cells [2]

Photodetectors [6]

Many of these functional properties are closely related to the features of the phonon spectrum and the electron-phonon interaction.
Notwithstanding a large number of studies of optical properties of hybrid perovskites, most of them were carried out on thin films. In this work, high quality large single crystals of methyl ammonia lead iodide ($CH_3NH_3PbI_3$) were investigated by high-resolution (up to 0.2 cm^{-1}) spectroscopy in the wide spectral (15 – 650 cm^{-1}, 1750 – 12000 cm^{-1}) and temperature (5 – 330 K) ranges.

$CH_3NH_3PbI_3$ structural phase transitions

[1]

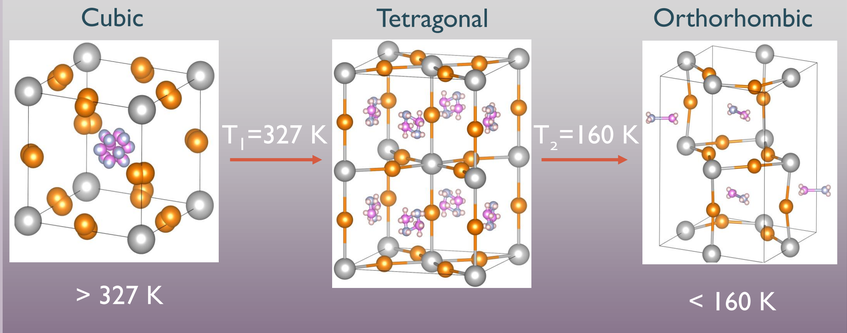

Three well-separated frequency regions of vibrations

[7]

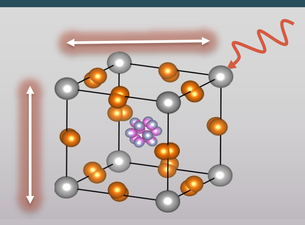

15 – 100 cm^{-1}
vibrations of the PbI_3 network consisting of heavy atoms and translational /librational modes of the MA cation

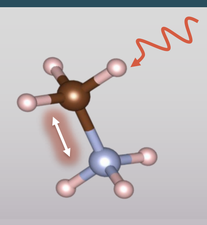

900–1600 cm^{-1}
CH_3NH_3 rocking modes, C–N stretching, and CH_3 and NH_3 bending vibrations

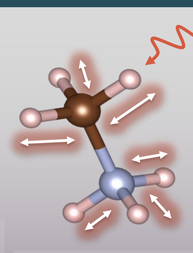

3000 and 3200 cm^{-1}
C–H and N–H stretching mode

In this work the reflection spectra in terahertz region and transmission spectra in the mid- and near-infrared (IR) regions of $CH_3NH_3PbI_3$ are studied for the first time for single crystals with the aim of obtaining information about low-frequency phonons and multiphonon lattice excitations that was not obtained by previously used experimental techniques or/and samples.

Sample preparation

[8]

1) CH_3NH_3I synthesis
2) PbI_2 synthesis

Two precursors

3) $CH_3NH_3I + PbI_2 \longrightarrow CH_3NH_3PbI_3$

Synthesized single crystals

Experimental setup

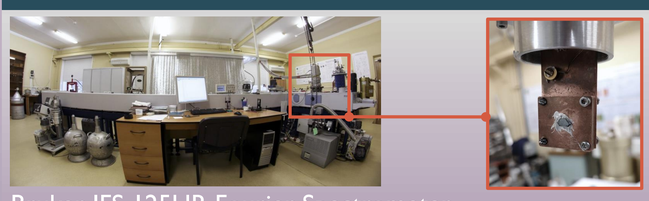

The sample on a cryostat copper finger

Bruker IFS 125HR Fourier Spectrometer

Registration of reflection and absorption spectra: Bruker IFS 125HR Fourier Spectrometer
Range: 10 - 30000 cm^{-1}
Resolution: up to 0.2 cm^{-1}
Sample cooling: CryoMech ST403 closed loop cryostat (Temperature range: 3.5-300 K)

Conclusions

- The high-resolution terahertz (far-IR) reflection and mid- and near-infrared transmission studies of $CH_3NH_3PbI_3$ hybrid perovskite single crystals were performed in a broad range of temperatures (5–350 K).
- We observed 13 new low-frequency modes not reported previously and investigated the multiphonon spectra for the first time.
- There are only two modes of the inorganic cage (with frequencies of about 30 and 60 cm^{-1}) that survive in all structural phases of $CH_3NH_3PbI_3$. Their frequencies do not change at the phase transition from the cubic to tetragonal phase (320 K) but experience an abrupt shift at the tetragonal to orthorhombic transition (160 K).
- A high sensitivity to the structural phase transitions and to changes in the rotational dynamics of the $CH_3NH_3^+$ molecular cation is demonstrated also by the multiphonon spectra.
- Splitting of selected multiphonon lines observed below the temperature of ~70 K (identified earlier with a transition to the tunneling dynamics) is tentatively assigned to the tunneling splitting.
- A complete melting of the orientational order above the temperature of the orthorhombic to tetragonal phase transition leads to a noticeable broadening of vibrational lines.

Reflection spectra

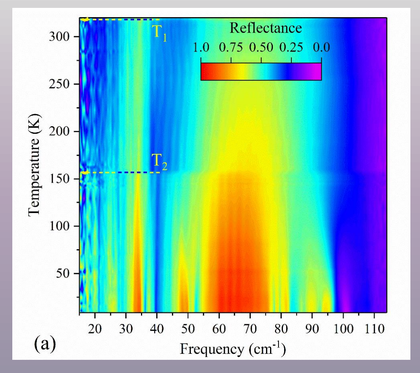

Reflection spectrum of a $CH_3NH_3PbI_3$ single crystal at 5 K (black lines) in the ranges (a) 15–400 cm^{-1} and (b) 15–160 cm^{-1}. A red dashed line is a result of simulation.

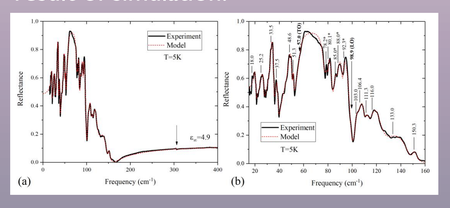

$$\varepsilon(\omega) = \varepsilon_\infty + \sum_{i=1}^{N} \frac{\omega_i^2 f_i}{\omega_i^2 - \omega^2 + i\omega\gamma_i}$$

$$R(\omega) = \left| \frac{\sqrt{\varepsilon(\omega)} - 1}{\sqrt{\varepsilon(\omega)} + 1} \right|^2$$

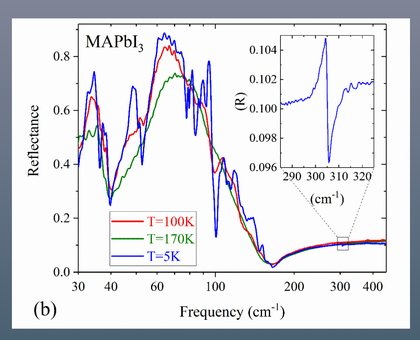

Reflection spectra of a $MAPbI_3$ single crystal (a) presented as the intensity map in the wave number – temperature axes and (b) at several selected temperatures.

The frequencies ω_{TO} and ω_{LO} of the optical modes, observed in the far-IR spectra of $MAPbI_3$ at 5 K. ε_∞ = 4.9, ε_0 = 27.5.

No	Ref. (10), 10 K ω_{TO} (cm^{-1})	This work, 5 K ω_{TO} (cm^{-1})	ω_{LO} (cm^{-1})	Tentative assignment
1	17	20.5	20.7	PbI_6 octahedra twist
2	22	26.6	27.3	PbI_6 octahedra twist
3	30	33.5	35.9	Pb–I–Pb rock
4	35	37.5	38.8	Pb–I–Pb rock
5	47	48.6	51.2	Pb–I–Pb bend
6	59	57.5	59.2	Pb–I–Pb stretch
7		78.0*	77.3	Pb–I–Pb bend
8		80.0*	79.6	Pb–I–Pb bend, $CH_3NH_3^+$ libr
9		85.9*	83.9	Pb–I–Pb bend, $CH_3NH_3^+$ libr
10		91.5*	91.3	$CH_3NH_3^+$ translation
11		92.8*	92.5	$CH_3NH_3^+$ translation
12		103.0	105.2	$CH_3NH_3^+$ libr/transl
13		106.3	110.0	$CH_3NH_3^+$ libr/transl
14		111.2	113.9	$CH_3NH_3^+$ rotation along C-N
15		116.0	126.1	
16		133.2	144.3	$CH_3NH_3^+$ libr/transl
17		150.1	152.6	$CH_3NH_3^+$ libr/transl
18		305.06	305.12	$CH_3NH_3^+$ torsion

* Inverted phonons

Multiphonon absorption spectra

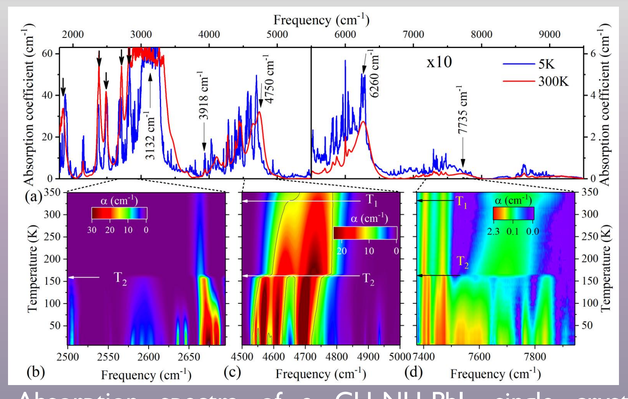

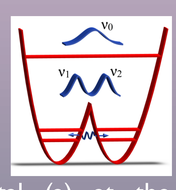

Absorption spectra of a $CH_3NH_3PbI_3$ single crystal (a) at the temperatures of 300 and 5 K (bold arrows mark two-phonon lines observed in the spectra of $CH_3NH_3PbI_3$ thin films [9]; thin arrows indicate lines discussed in our work [11]). (b–d) Color intensity maps in the frequency–temperature axes for selected frequency regions. In (b), the contribution from the strong band at about 3000 cm^{-1} is subtracted. Temperatures T_1 and $T_2$2 of the structural phase transitions are marked by horizontal arrows.

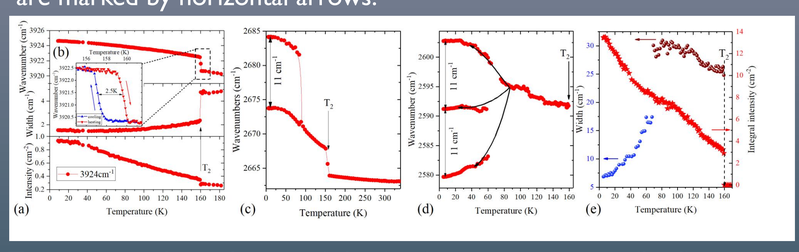

Temperature dependences of the (a, e) integral intensity, (b–d) position, and (b, e) FWHH for (a, b) a singlet 3918 cm^{-1}, (c) a doublet near 2680 cm^{-1}, and (d, e) a triplet near 2600 cm^{-1}. Below 70 K, the width of the central component of the triplet is presented. The inset (b) shows a hysteresis for the line position at cooling and heating a $CH_3NH_3PbI_3$ single crystal.

References

[1] M. R. Filip, Handbook of Materials Modeling (Springer, Cham), 1, (2018).
[2] T. Brenner, D. Egger, L. Kronik, G. Hodes, D. Cahen, Nat. Rev. Mater. 1, 15007 (2016).
[3] NREL https://www.nrel.gov/pv/cell-efficiency.html.
[4] Z.-K. Tan, R. S. Moghaddam, M. L. Lai, et al., Nature Nanotech 9, 687–692 (2014).
[5] A. Zhizhchenko, S. Syubaev, A. Berestennikov, et al., ACS Nano 13, 4, 4140, (2019).
[6] Z. Lian, Q. Yan, Q. Lv, et al., Scientific Reports, 5, 16563 (2015).
[7] F. Brivio, J. M. Frost, J. M. Skelton, et. al., Phys. Rev. B: Condens. Matter Mater. Phys., 92, 144308, (2015).
[8] O. Semenova, E. Yudanova, N. Yeryukov, et al., J. Cryst. Growth 462, 45 (2017).
[9] T. Glaser, C. Müller, M. Sendner, et al., J. Phys. Chem. Lett. 6, 2913 (2015).
[10] M. A. Perez-Osorio, R. L. Milot, M. R. Filip, et. al., J. Phys. Chem. C, 119, 25703, (2015).
[11] K. Boldyrev, V. Anikeeva, O. Semenova, M. Popova, J. Phys. Chem. C, 124, 42, 23307 (2020).

Acknowledgments

RSF Russian Science Foundation

This work was supported by the Russian Science Foundation (Grant No.19-72-10132).